4 3 42

Reprinted from JOURNAL OF APPLIED PHYSICS, Vol. 35, No. 6, 1956–1959, June 1964

Three-Dimensional X-Ray Topographic Studies of Internal Dislocation Sources in Silicon*

A. AUTHIER† AND A. R. LANG
H. H. Wills Physics Laboratory, University of Bristol, England
(Received 8 October 1963)

Stereo pairs of x-ray projection topographs have been used to elucidate the configuration of dislocations in a silicon bar lightly deformed at about 900°C. Dislocation reactions and interactions associated with a ten-turn Frank–Read spiral are described.

INTRODUCTION

IN 1950 Frank and Read[1] proposed mechanisms which could produce an unlimited increase of dislocation line length in crystals undergoing plastic deformation. Direct confirmation of their ideas had to await the development of techniques for making dislocations visible within the interior of crystals. Internal dislocation sources clearly exhibiting the configurations predicted by Frank and Read were first revealed by Dash, using his copper precipitation technique for rendering dislocations in silicon observable by infrared transmission microscopy.[2,3] Dash's pictures showed in spectacular fashion both the multi-turn spiral produced when the dislocation has a single anchor point and the symmetrical source of closed loops formed when the dislocation has a pair of anchor points on its slip plane. Further work, using decoration, electron microscopic, and x-ray topographic techniques applied to a wide variety of crystals, has shown that the ideal Frank–Read dislocation mill is something of a rarity. Under usual conditions of plastic deformation the lack of stable pinning of the anchor points and the interference from other dislocations prevent any single source from operating repetitively more than a few times. Moreover, surface sources generally predominate over internal sources in the initial stages of dislocation multiplication in nearly perfect crystals. The ideal internal Frank–Read source is, however, a feature worthy of study. It is of interest to examine the dislocation conditions that bring it into action, and the circumstances that subsequently cause its operation to cease. X-ray topography is an appropriate technique to use in such an investigation for the following reasons: (1) the specimen must be sufficiently thick so that the operation of the internal source is not appreciably influenced by surface effects; (2) the density of dislocations encountered falls within the compass of the x-ray methods since the study must, of necessity, be made in the initial stages of plastic deformation of a fairly perfect crystal; (3) Burgers vectors of dislocations must be determined; (4) the x-ray projection topograph[4] gives an orthographic projection of the whole specimen volume and does not suffer from the limited depth of focus of the optical microscope used in examining decorated crystals; and (5) the three-dimensional configuration of dislocations can be determined from stereo pairs of projection topographs, supplemented, if need be, by section topographs.[5] An additional advantage of the x-ray method is that the x-ray examination may be repeated as often as desired. This facility has been used by Gerold and Meier[6,7] who have taken sequences of x-ray topographs of germanium to show the multiplication and movement of dislocations under repetitive stressing of the specimen.

FIG. 1. Projection topograph showing spiral deep inside crystal, $02\bar{2}$ reflection, scale mark 100μ.

* Research supported by the Aeronautical Research Laboratory, OAR, through the European Office, Aerospace Research, U. S. Air Force.

†Present address: Laboratoire de Physique Théorique, Collège de France, 11, Place Marcelin Berthelot, Paris V^e.

[1] F. C. Frank and W. T. Read, Phys. Rev. **79**, 722 (1950).
[2] W. C. Dash, J. Appl. Phys. **27**, 1193 (1956).
[3] W. C. Dash in *Dislocations and Mechanical Properties of Crystals*, edited by J. Fisher (John Wiley & Sons Inc., New York, 1957), p. 57.
[4] A. R. Lang, Acta Cryst. **12**, 249 (1959).
[5] A. R. Lang, Acta Met. **5**, 358 (1957).
[6] V. Gerold and F. Meier in *Direct Observation of Imperfections in Crystals*, edited by J. B. Newkirk and J. H. Wernick (Interscience Publishers, Inc., New York, 1962), p. 509.
[7] F. Meier, Z. Physik **168**, 29 (1962).

EXPERIMENTAL PROCEDURE

The x-ray topographic studies were performed on lightly deformed silicon specimens prepared by the late W. C. Dash to whom the authors are greatly indebted. The specimen described here was a rectangular bar, 2.8×3.3 mm in section. The axis of the bar was normal to one of the octahedral slip-planes, and was designated [111]. The side faces of the bar were the pair (1$\bar{1}$0), ($\bar{1}$10), 3.3 mm wide, and the pair (11$\bar{2}$), ($\bar{1}\bar{1}$2), 2.8 mm wide. The bar had been twisted about its long axis at approximately 900°C, with a stress sufficient to cause fracture. Away from the regions that had been gripped in the chucks holding the specimen during stressing, slip had occurred mainly on the plane normal to the bar axis, i.e., (111), and at four points in the 10-mm length between the disturbed gripped region and the fracture, a high density of dislocations was found on these slip planes. Some slip had also occurred on the octahedral planes making 19½° with the bar axis, and at a few places on these a high local dislocation density was reached. The x-ray topographs showed that the overwhelming majority of dislocations had run into the

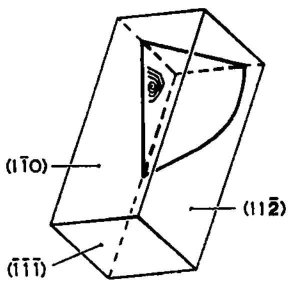

FIG. 2. Relationship of pyramidal specimen to bar from which it was cut.

crystal from surface sources, and the indications were that this specimen had been dislocation-free before deformation. The twisting had been performed under conditions which give straight dislocation segments parallel to <110>. Such conditions also favour the production of Frank–Read sources which can continue in operation for more than a few turns. The best developed internal source in this specimen is shown in the x-ray topograph Fig. 1. An interesting feature of this source is that there is a baby source on one turn of the main spiral. To facilitate study, the part containing the spiral of Fig. 1 was cut away from the bar by slicing with a wire saw. The cut was made in the plane parallel to the main spiral and about half a millimeter distant from it. Figure 2 shows the relationship between the original bar and the piece cut away. The latter has roughly the shape of a flat pyramid, its base being (1$\bar{1}\bar{1}$), the plane of the main spiral, and the three sides meeting at its apex being (111), ($\bar{1}$10), and ($\bar{1}\bar{1}$2). During x-ray topographic examination this pyramidal specimen was always mounted so that the plane (1$\bar{1}\bar{1}$) contained both the goniometer axis and the direction of specimen traverse used in taking the projection topograph. The apex of

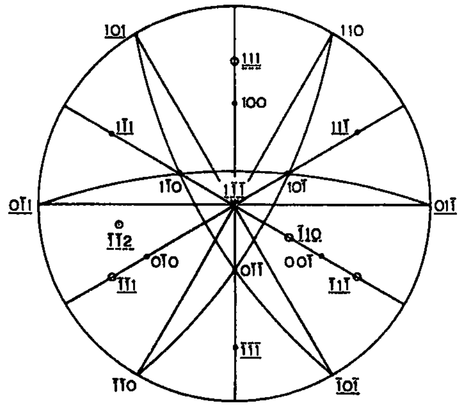

FIG. 3. Stereographic projection on (1$\bar{1}\bar{1}$) face of pyramidal specimen. Circles indicate points in lower hemisphere.

the pyramid pointed towards the x-ray source so that the exit surface for x rays diffracted through the specimen was always the (1$\bar{1}\bar{1}$) face. Thus a stereographic projection on (1$\bar{1}\bar{1}$) is useful for interpreting the topographs and is shown in Fig. 3. On this projection the faces of the specimen are indicated by dotted lines under the index and the planes used for topograph reflections are underlined solid. The important diagnostic reflections for determining Burgers vectors in the diamond structure are those from {111} planes. Entire topographs of the $\bar{1}1\bar{1}$ and $1\bar{1}1$ reflections are shown in Figs. 4 and 5(a), respectively. These and other topographs readily show that the spiral dislocation (hereafter called dislocation A) has Burgers vector parallel to [110]. Dislocations with five out of the six possible Burgers

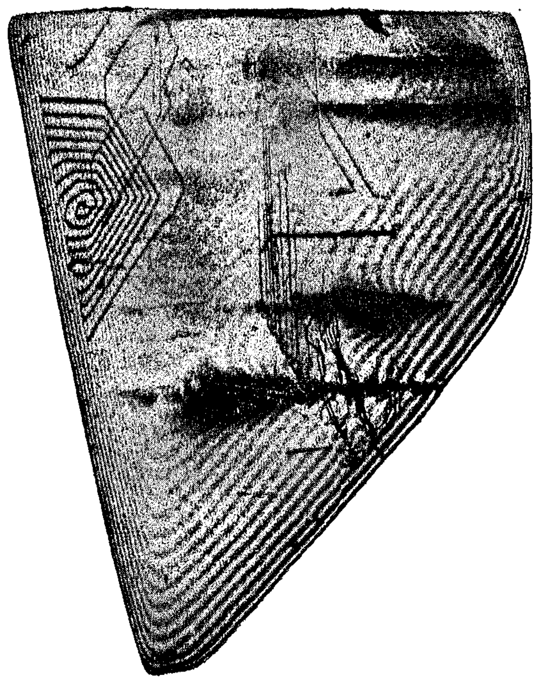

FIG. 4. Projection topograph, $\bar{1}1\bar{1}$ reflection.

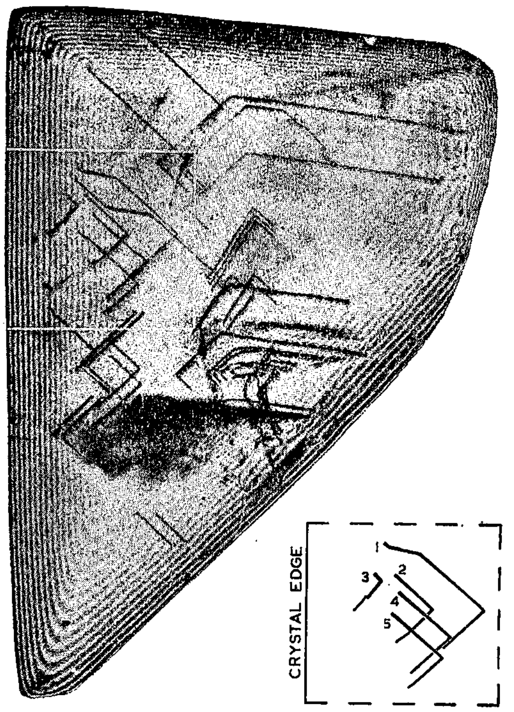

(a) (b)

FIG. 5(a) Projection topograph, $1\bar{1}1$ reflection; (b) key to numbered B dislocations in region outlined on (a).

vectors in <110> directions show up in 220-type reflections. Hence these latter reflections are useful for displaying the complete dislocation configuration. For example, Fig. 6, which is part of the $0\bar{2}2$ topograph, shows the dislocations appearing in both Fig. 4 and Fig. 5(a) in the region of the spiral A. Pairs of reflections from an octahedral plane and its inverse are the most useful for steroscopic viewing.[8] Figure 7 shows part of the 111 topograph, and parallax between it and the $\bar{1}\bar{1}\bar{1}$

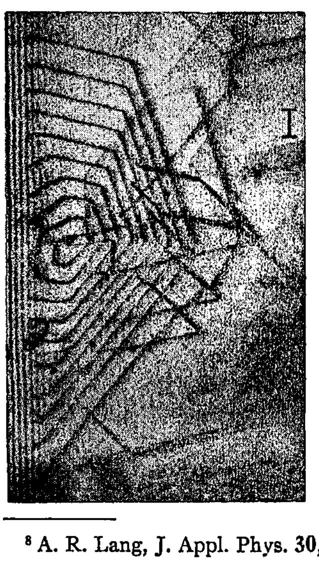

FIG. 6. Part of $0\bar{2}2$ topograph, scale mark $100\,\mu$.

[8] A. R. Lang, J. Appl. Phys. 30, 1748 (1959).

topograph (Fig. 4) in the field common to both is easily noticeable. After it had been cut from the bar the specimen was thoroughly etched to remove surface damage. The thickness of the layer removed from the $(\bar{1}\bar{1}2)$ surface was as much as 80μ, which accounts for the different amount of the main spiral and baby source seen in Fig. 1 compared with later topographs.

INTERPRETATION AND DISCUSSION

A cursory inspection of the topographs suffices to show that the spatial relationships between dislocations are quite complicated, even at the low dislocation density present in the region of the spiral. We will deal here with the interpretation of the configuration of this region. Other features evident in Figs. 4 and 5(a), such as the long-range strains due to dislocations piling up on some of the (111) planes, the diffraction contrast given by these strains and their bending effect on

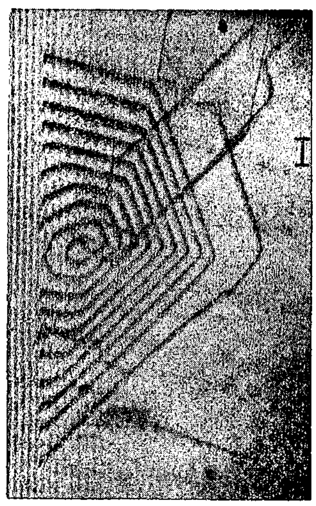

FIG. 7. Part of 111 topograph, scale mark $100\,\mu$.

Pendellösung fringes [9,10] will be considered separately.[11]

In the region of the spiral we see dislocations on three slip planes: $(1\bar{1}\bar{1})$, $(1\bar{1}1)$, and (111). In this part of the specimen some single dislocations, each lying on a different (111) plane, have invaded the crystal from the $(\bar{1}\bar{1}2)$ face. Five such dislocations can be seen, by stereoscopic examination, to be in contact with the spiral dislocation A. They are numbered B_1 to B_5 and may be identified on the topograph Fig. 5(a) with the aid of the drawing Fig. 5(b). The unnumbered dislocation outcropping between B_1 and B_2 runs very close to the spiral but appears not to be in contact with it. The Burgers vectors of the B dislocations are parallel to $[01\bar{1}]$. The main spiral has segments parallel to [110], $[01\bar{1}]$ and $[\bar{1}0\bar{1}]$. Pure screw dislocations are strictly invisible in reflections from planes containing their Burgers vector,

[9] N. Kato and A. R. Lang, Acta Cryst. 12, 787 (1959).
[10] N. Kato, Acta Cryst. 16, 282 (1963).
[11] A. Authier and A. R. Lang (to be published).

but 60° dislocations do not vanish. Of the B dislocations numbered, only B_1 has a pure screw segment (parallel to $[01\bar{1}]$) within this specimen; all their other segments appearing in the topographs are of 60° type. Consequently we can see these 60° dislocations faintly on the 111 (Fig. 7) and $\bar{1}\bar{1}\bar{1}$ (Fig. 4) topographs. Their location with respect to dislocation A is indicated on Fig. 8, which is drawn for the direction of view corresponding to the $\bar{1}\bar{1}\bar{1}$ topograph. The two octahedral planes on which parts of dislocation A lie, $(1\bar{1}1)$ and $(1\bar{1}\bar{1})$, are shown as intersecting sheets. Part of the $(1\bar{1}\bar{1})$ sheet is cut away to display better the segments of A lying on the $(1\bar{1}1)$ plane. No (111) planes are drawn in Fig. 8, but to indicate spatial relations the parts of the B dislocations which are above the plane of the spiral are shown as solid lines and the parts below as interrupted lines. Shown by the dotted line in Fig. 8 is the single dislocation C lying deep below A and having similar Burgers vector to A. The anchor point of the spiral has not moved detectably during the operation of ten turns of the spiral. On the other hand, the free end of A, lying on its original slip-plane $(1\bar{1}1)$, has extended in length and now forms two large loops, roughly in the shape of elongated hexagons. This movement may have taken place simultaneously with the operation of the spiral, but more probably happened later. Dislocation A crosses over itself at X, but the separation of the two segments where they cross is too small to measure on the topographs. At Y the two loops on $(1\bar{1}1)$ approach each other within 25 μ. The present nearer loop on $(1\bar{1}1)$ and several turns of the spiral on $(1\bar{1}\bar{1})$ have cut through each other without apparent interaction. The direction of elongation of hexagonal loops seen in the specimen indicates that the 60° segments have travelled faster than the pure screw segments.

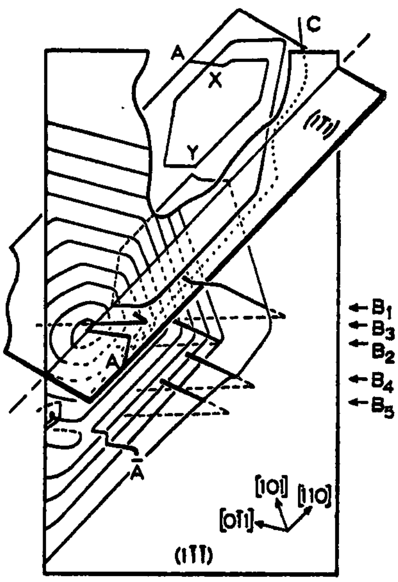

FIG. 8. Dislocation configuration in vicinity of spiral. Letters A indicate outcrops of dislocation A at near and far specimen surfaces. Arrows point towards intersections of B dislocations with plane of spiral.

Considering next the B dislocations due to slip on (111), it appears likely that B_1, B_4, and B_5 have pushed the outermost turn of the spiral some distance into the crystal. At its contact with A, dislocation B_4 has produced a jog about 15 μ long and parallel to $[01\bar{1}]$. The present topographic experiments give only the direction and not the sense of Burgers vectors (though determination of sense as well as direction is possible under suitably chosen diffraction conditions[12]). However, the examination of dislocation interactions gives an idea of the relative senses of Burgers vectors. For example, if we take the Burgers vector of A to be in the direction $[110]$ (including sense), then the Burgers vector of the B dislocations could be in the direction $[01\bar{1}]$ or its inverse $[0\bar{1}1]$. In the latter case the reaction $\frac{1}{2}[110]+\frac{1}{2}[0\bar{1}1]=\frac{1}{2}[101]$ would be possible, and the jog where A and B_4 meet would be expected to have this combination Burgers vector. The topographs indicate that the above reaction has not taken place, and so we take the B Burgers vector to be in the direction $[01\bar{1}]$, the angle between the A and B Burgers vectors thus being 60° rather than 120°. A clear indication of relative sense of Burgers vector is given by the dislocation $\bar{A}$ (seen in the topographs of Figs. 4, 6, and 7 and drawn in Fig. 8). Its visibility behavior is the same as that of dislocation A, but its annihilation reaction where it meets A shows that it has opposite sense. The dislocation configuration observed in the vicinity of the spiral gives no clue as to why the source stopped functioning, but it is reasonable to suppose that slip occurring elsewhere in the crystal, either on the main (111) slip planes normal to the axis of twist or on other planes oblique to the axis, caused the local stress on this oblique $(1\bar{1}\bar{1})$ plane to drop below the yield value. Finally we come to consider the baby source. The topographs show that no other dislocation besides A is involved in its genesis. It is expanding on the $(1\bar{1}1)$ plane and has arisen through cross slip of a short $[110]$ segment in the side of the hexagon nominally parallel to $[01\bar{1}]$. With regard to the directions of dislocation lines, it may be noted that the departures from strict orientation along $<110>$ axes can amount to several degrees in this specimen. Compare, for example, the $[10\bar{1}]$ segments of dislocations A and B_3, and the $[110]$ segments of dislocations A and C. Also, the corners of the hexagons are noticeably rounded off, with radii between 20 and 40 μ.

[12] M. Hart and A. R. Lang, Sixth Intern. Cong. Cryst., Rome, 1963, Paper 12.4.